Enhancing the mechanical and *in vitro* performance of robocast bioglass scaffolds by polymeric coatings: Effect of polymer composition

Azadeh Motealleh, Siamak Eqtesadi, Antonia Pajares, Pedro Miranda*

Departamento de Ingeniería Mecánica, Energética y de los Materiales,

Universidad de Extremadura, Escuela de Ingenierías Industriales,

Avda. de Elvas s/n, 06006 Badajoz, Spain.

* Corresponding author.

Pedro Miranda's contact details:

Email: pmiranda@unex.es

Phone: + 34 924 289 300 Ext: 86735.

Fax: + 34 924 289 601

Address: Escuela de Ingenierías Industriales,

Avda. de Elvas s/n,

06006 Badajoz, Spain

Abstract

The effect of different polymeric coatings, including natural and synthetic compositions, on the mechanical performance of 45S5 bioglass robocast scaffolds is systematically analyzed in this work. Fully amorphous 45S5 bioglass robocast scaffolds sintered at 550 °C were impregnated with natural (gelatin, alginate, and chitosan) and synthetic (polycaprolactone, PCL and poly-lactic acid, PLA) polymers through a dip-coating process. Mechanical enhancement provided by these coatings in terms of both compressive strength and strain energy density was evaluated. Natural polymers, in general, and chitosan, in particular, were found to produce the greater reinforcement. The effect of these coatings on the *in vitro* bioactivity and degradation behavior of 45S5 bioglass robocast scaffolds was also investigated through immersion tests in simulated body fluid (SBF). Coatings from natural polymers, especially chitosan, are shown to have a positive effect on the bioactivity of 45S5 bioglass, accelerating the formation of an apatite-like layer. Besides, most coating compositions reduced the degradation (weight loss) rate of the scaffold, which has a positive impact on the evolution of their mechanical properties.

Keywords: 45S5 Bioglass, polymer coating, robocasting, mechanical properties.

1. Introduction

Application of polymeric coatings onto bioceramics scaffolds is gaining increasing attention within the biomaterials community (Philippart et al., 2015). One of the main reasons for applying polymeric coatings onto bioceramic scaffolds lies in the mechanical enhancement they can provide, both in terms of strength and toughness (Eqtesadi et al., 2015; Martínez-Vázquez et al., 2014, 2013a; Peroglio et al., 2007). Strengthening effect in coated structures is produced by a defect healing mechanism, which means that the infiltration of the micropores or microcracks on the scaffold struts by the polymer makes it harder to initiate a crack from them (Eqtesadi et al., 2015; Martínez-Vázquez et al., 2013a, 2013b, 2010). On the other hand, a toughening effect is provided by polymeric fibrils that bridge the crack walls together during crack propagation, which need to be stretched and eventually broken for the propagation to continue (Martínez-Vázquez et al., 2014; Peroglio et al., 2007). The extent of such reinforcing effect will depend on the mechanical properties of the polymer, the quality of the polymer infiltration and the conditions at the polymer–ceramic interface (Martínez-Vázquez et al., 2013a; Philippart et al., 2015). Although processes like *in situ* polymerization (Martínez-Vázquez et al., 2013a, 2013b) may offer advantages in terms of interfacial strength, dip-coating process has received considerable attention for the deposition of such reinforcing coatings due to its simplicity and versatility, which facilitates the use of a diversity of polymer compositions in order to meet the clinical demands (Roether et al., 2002). Some important parameters involved in this process that can affect the polymeric coating performance such as polymer concentration, solvent composition and deposition temperature have been systematically studied in a previous work (Motealleh et al., 2016). In that study, it was shown that while the mechanical performance of ceramic/polymer hybrid scaffolds improves monotonically with the polymer concentration in the

starting solution, this concentration cannot be increased indefinitely if the pore interconnectivity is to be preserved. An optimal concentration exists for any given set of process variables (scaffold geometry and material, polymer, solvent and process temperature) that yields coatings with optimal reinforcement and minimal reduction of scaffold functionality.

However, which is the best polymer composition to be used in this reinforcement strategy for a particular substrate still remains unclear. There are indeed multiple choices for coating and impregnation of different types of bioceramic and bioactive glass scaffolds with synthetic polymers, including synthetic polymers like PCL, PDLLA and PLGA, or PHB (Philippart et al., 2015) and natural polymers such as silk (Wu et al., 2010), chitosan (Govindan et al., 2015), gelatin (Metze et al., 2013), collagen (Chen et al., 2008), and alginate (Erol et al., 2012). Synthetic polymeric coatings can have potentially better intrinsic mechanical performance but require the use of organic solvents in the fabrication process, whose remnants may be harmful to cells or host tissues (Li et al., 2013). Thus, natural polymers are becoming more widely used to coat bioceramic scaffolds in order to avoid the use of potentially toxic organic solvents in the fabrication of these composite scaffolds. However, one may expect that such increased safety will come at the expense of the mechanical performance.

In this study, a comparative analysis of the effectiveness of different polymeric coatings as reinforcements of 45S5 Bioglass® robocast scaffolds is performed. 45S5 bioglass was selected as the scaffold material since it has been widely analyzed and successfully used as bone graft substitute in clinical applications (Gerhardt and Boccaccini, 2010; Jones, 2013). Although there have been many reports on the improvement of mechanical properties of 45S5 bioglass scaffolds by both synthetic (Bretcanu et al., 2007; Chen and Boccaccini, 2006; Li et al., 2014a) and natural (Li et al., 2014b; Metze et al., 2013; Yang et al., 2012) polymeric coatings, no systematic

comparison on reproducible substrates exists in the literature. The use of an additive manufacturing technique such as robocasting, unlike other conventional alternatives, enables the fabrication of scaffolds with a controlled internal pore architecture and strut morphology (and external geometry, if necessary), which are especially suitable for that purpose. Furthermore, robocasting technique — a 3D printing method consisting on the robotic deposition of concentrated suspensions (Cesarano et al., 1998; Cesarano III, Joseph; calvert, 2000; Miranda et al., 2006) — can also produce 45S5 bioglass scaffolds with compressive strengths that are far superior to any previously reported values, which allow one to produce fully amorphous structures by sintering at low temperature (550 °C) (Eqtesadi et al., 2016, 2014), as is done in this study. Three natural (gelatin, alginate, and chitosan) and two synthetic (PCL and PLA) polymers — chosen for being among the most widely used biopolymers in bone tissue engineering — will be deposited onto these amorphous 45S5 bioglass scaffolds by a dip-coating process in order to systematically analyze the effect of the different polymeric coating compositions on the mechanical and biological performance of these scaffolds. The latter will be analyzed through tests of immersion in simulated body fluid (SBF), for determining *in vitro* bioactivity and degradation behavior. Dip-coating was selected as the coating method due to its simplicity and low cost, which makes it one of the most widely used coating procedures for applying homogeneous polymeric films onto scaffolds (Motealleh et al., 2016).

2. Materials and methods

2.1. Fabrication of 45S5 bioglass scaffolds

Bioglass powder with 45S5 composition —45% SiO_2, 24.5% CaO, 24.5% Na_2O and 6% P_2O_5 (wt.%)— was supplied by MO-SCI Corporation (USA). 45S5 bioglass scaffolds were

prepared by robocasting technique following a procedure described in detail elsewhere (Eqtesadi et al., 2014, 2013a). Briefly, a suspension of milled 45S5 bioglass powder (average size ~ 4 μm) with a concentration around 45 vol.% was prepared using 1 wt.% carboxymethyl cellulose (CMC, Lamberti Iberia. S.A.U., Castellón, Spain) as the sole organic additive. As schematically shown in Figure 1a, the resulting ink was housed in a syringe and extruded through a conical nozzle (inner diameter, d = 410 μm), and used to fabricate three-dimensional scaffolds of 45S5 bioglass layer-by-layer with the aid of a robocasting device (A3200, 3D inks, Stillwater, OK, USA). After deposition, the samples were removed from the oil bath used to prevent non-uniform drying during printing, and dried in ambient conditions for at least one day. The samples were then debinded at 400 °C for 1 h and sintered at 550 °C to obtain fully amorphous 45S5 bioglass scaffolds (Eqtesadi et al., 2014). Although minor changes in composition (e.g. impurities from powder milling and loss of alkaline species through dissolution during ink preparation) could have occurred during this fabrication process, all the main characteristics of the 45S5 bioglass are preserved, as demonstrated in previous studies (Eqtesadi et al., 2014, 2013b)

2.2. Polymer coating procedure

The amorphous 45S5 bioglass scaffolds were coated with different polymers by the dip-coating process, i.e. by immersing them in a polymer solution (Figure 1b). For this purpose, two synthetic polymers, PCL (Capa™ 6500, Perstorp, UK) and PLA (ICO Polymers, Ecorene™ NW61-100), and three natural polymers, gelatin from porcine skin (G2500, Sigma Aldrich), sodium alginate (W201502, Sigma Aldrich), and chitosan (85/20, Heppe Medical Chitosan GmbH, Germany), were used. Polymer solutions were prepared by slowly adding the as-received

polymer to the appropriate solvent at 60 °C and stirring constantly until full dissolution. Both synthetic polymers were dissolved in toluene (puriss. p.a., Sigma Aldrich), alginate and gelatin were dissolved in distilled water and chitosan was dissolved in a 2 vol.% acetic acid aqueous solution. According to previous works (Eqtesadi et al., 2016; Motealleh et al., 2016), the optimal solution concentrations—which maximize mechanical strength while preserving pore interconnectivity—for the preparation of PCL and PLA coatings in toluene at 60 °C are 25 % and 15 % (w/v), respectively. For all natural polymers, the maximum concentration that could be successfully used in order to avoid clogging of the scaffolds macropores was 5 % (w/v). For comparative purposes, scaffolds coated with PCL and PLA were prepared both at the aforementioned optimal concentrations and at the same concentration used for the natural polymers, 5 % (w/v). Dip-coating was performed in air by placing the bioglass scaffolds in the indicated polymer solutions at 60 °C for 30 min under mild stirring. Coated scaffolds were then retrieved and kept in an oven at 37 °C for 48 h to evaporate the solvent.

2.3. Characterization methods

The microstructure of scaffolds before and after coatings was observed using a scanning electron microscopy (SEM, S-3600N, Hitachi, Japan), after metallization in a sputter-coater. When required, cross-sectional images were obtained from fracture surfaces or scaffolds specimens previously cut with a diamond blade.

The mechanical response of the scaffolds was evaluated by uniaxial compression. Compressive tests were performed in air using a universal testing machine (AG-IS 10KN, Shimadzu Corp., Kyoto, Japan). Nine parallelepipedic specimens with external dimensions of 3 × 3 × 6 mm were cut with a diamond blade in an automatic cutting machine (Accutom-50,

Struers, Denmark) from each type of polymer-coated ceramic structures, as well as for the as-sintered scaffolds, for testing. The force was applied perpendicular to the printing plane (i.e. orthogonal to the scaffold rods) at a constant crosshead speed of 0.6 mm min^{-1}. The compressive strength of each type of scaffold was evaluated as the average maximum stress applied during the tests, and the toughness (strain energy density) as the mean area under the corresponding stress-strain curves up to 20 % strain.

2.4. Biodegradation study by immersion in simulated body fluid

The *in vitro* bioactivity, degradation and mechanical properties evolution of 45S5 bioglass scaffolds after coatings were investigated by soaking them in simulated body fluid (SBF), following the same procedure as in a previous study on the bare scaffolds (Motealleh et al., 2017). The SBF solution was prepared according to the procedure described by Kokubo (Kokubo and Takadama, 2006). Scaffolds, with dimensions of 3 × 3 × 6 mm, were immersed in polyethylene bottles containing SBF solution at a liquid/solid ratio of 100 ml/g, and kept in an incubator at 37 °C for up to 8 weeks, without shaking. The SBF solution was refreshed once during the experiment (after 4 weeks). The evolution of sample weight, solution pH, surface mineralization and mechanical properties with immersion time were evaluated for each type of sample.

Scaffold weight loss during immersion in the SBF solution was calculated as $\Delta W/W_0$, where $\Delta W=W_0-W_t$, W_0 is the initial mass of the scaffold, and W_t is the mass at time t. At the end of each time point, the scaffolds were removed from the SBF solution, then rinsed with distilled water and dried at 37 °C for 24 h, and eventually their final weight (W_t) was carefully measured. For each time point, three scaffolds of each material were used to measure the weight loss, and

the results were presented as mean with standard deviation as error. Evolution of the SBF solution's pH was measured on separate specimens, using two samples per material and time point. After retrieving these scaffolds, the SBF solution was cooled to room temperature, and the pH was measured.

The surface morphology of scaffolds after SBF immersion was observed by SEM to analyze the progress of surface mineralization. Identification of the crystalline phases deposited onto the scaffolds was done by X-ray diffractometry (XRD, Bruker D8 ADVANCE, USA) using CuKα_1 radiation (step width 0.03° 2θ, angular interval 20–70° 2θ, and count time 2 s per step) on samples immersed on the SBF for 8 weeks.

To evaluate the evolution of the scaffolds' mechanical properties with immersion time separate samples were used for compressive tests. A minimum of 9 samples per material and time point were tested in uniaxial compression, following the procedures described above.

3. Result and discussion

3.1. Microstructural characterization

In order to illustrate the morphology of the robocast 45S5 bioglass scaffolds analyzed in this study, Figure 2 shows a representative SEM micrograph of a chitosan-coated structure. As shown in this figure, the scaffolds consist of a network of inter-penetrating rods (d = 359 ± 9 μm) with tetragonal symmetry and a pre-designed volumetric macroporosity of around 50 %. As can be seen, the macroporosity remains unclogged after the coating process, not only for chitosan but also for the rest of polymeric coatings analyzed, which are not shown here since, at this magnification all exhibit very similar features.

The differences between the various scaffolds analyzed in this work become more evident, however, at higher magnifications. Figure 3 displays representative SEM micrographs of rod surfaces of bioglass scaffolds sintered at 550 ºC before and after coating with all the investigated polymers using optimally concentrated solutions. The bare scaffold (Fig. 3a), sintered at 550 ºC, is fully amorphous and very porous (24 ± 7% in-rod microporosity) (Eqtesadi et al., 2014). After dip-coating, the strut surfaces are covered with the polymers, which fill almost completely—with the exception of gelatin (Fig. 3d)—the surface micropores. The polymer-coated rods are not, however, totally smooth and the roughness of the original struts is still apparent in spite of the polymer coat.

Analogously, Figure 4 shows the corresponding micrographs of transversal fracture surfaces of 45S5 bioglass scaffold struts with and without polymeric coatings. Polymer is visible within the internal microporosity of the struts in all coated structures, although apparently less abundant in the case of gelatin (Fig. 4d). However, most composite structures seem to fracture in a somewhat brittle manner, as did the bare samples, and stretched polymeric fibrils generated during fracture are only apparent in the scaffolds coated with chitosan (Fig. 4c) and PCL (Fig. 4f).

3.2. Mechanical characterization

Figure 5 shows the effect of the different polymeric coatings on the compressive strength (Fig. 5a) and strain energy density (Fig. 5b) of the bioglass scaffolds. Data for synthetic polymers is provided for both coatings deposited using a solution concentration similar to that used for the natural polymers, 5 % (w/v), and the optimal concentration for each synthetic polymer, 25 % (w/v) for PCL and 15 % (w/v) for PLA. The mechanical enhancement over the

bare scaffolds provided by polymeric coating both in terms of strength and, especially, toughness is evident. As already mentioned in the introduction, the strengthening of polymer-coated scaffolds (Fig. 5a) is attributed to a defect healing mechanism (Eqtesadi et al., 2015; Martínez-Vázquez et al., 2013a, 2013b, 2010). The improvement in toughness (Fig. 5b), which is considerably greater than the strengthening produced—even the weakest PCL-coatings enhance toughness almost by an order of magnitude (toughening factor of ~ 7.6)—, results both from the strengthening provided by the polymer and from a crack bridging mechanism associated to the formation of polymeric fibrils (Martínez-Vázquez et al., 2014; Peroglio et al., 2007). Scaffolds infiltrated by natural polymers exhibit greater strength (Fig. 5a) and toughness (Fig. 5b) than those coated with the two synthetic compositions, especially when the same concentration of the starting solution is used for the dip-coating process.

The fact that this occurs despite the presumably superior intrinsic mechanical properties of both synthetic polymers, seems to corroborate the existence of a deleterious chemical interaction between the 45S5 bioglass and PCL and PLA polymers, as evidenced in previous works (Eqtesadi et al., 2016, 2015). Among the natural polymers, chitosan-coated structures exhibited the highest strengthening and toughening effects, with around a 6-fold and 25-fold increase, respectively, over the bare scaffolds. The good level of infiltration of the struts microporosity achieved with this polymer (Fig. 3c), together with its ability to generate microfibrils for crack bridging (Fig. 4c), explain its outstanding performance as a reinforcing coating for 45S5 bioglass robocast scaffolds. Gelatin seem unable to produce the same level of infiltration, which is attributed to an increase in viscosity and turbidity of gelatin solution upon immersion of the 45S5 bioglass scaffolds as the pH increases due to its fast dissolution. This phenomenon is considered to be linked to denaturation of collagen molecules at this high pH

values. However despite the poor level of infiltration of gelatin, this coating produces a similar level of reinforcement as alginate or the synthetic polymers. This can be attributed to either stronger intrinsic mechanical properties or enhanced interfacial adhesion between gelatin and the bioglass —indeed, strong (ionic) chemical bonds can form between the –COOH and –NH^2 groups in the gelatin and the silanol (Si-OH) groups of the 45S5 bioglass.

A strong interfacial adhesion can also be key to the outstanding performance of chitosan coatings. 45S5 bioglass–chitosan composites have been shown to exhibit excellent interfacial adhesion, thanks to hydrogen bonding between the Si-OH groups in the glass and the C=O and N–H groups of chitosan, as well as electrostatic (ionic) interactions (Al-Sagheer and Muslim, 2010; Oudadesse et al., 2011; Rashidova et al., 2004). On the other hand, interfacial bonding between 45S5 bioglass and the less polar synthetic polymers is significantly less favorable, which might also contribute to the lower level of reinforcement they provide. The C=O groups of PCL and PLA capable of forming hydrogen bonds with the silanol surface groups in the inorganic network (Allo et al., 2010) are less abundant in the case of PCL— the chain ratio between the methylene non-polar groups (-CH_2-) and the ester polar groups (C=O), is of 5:1, *vs.* 2:1 for PLA— which can explain why PLA exhibits a slightly higher strengthening effect than PCL (especially at 5 % w/v), despite being more susceptible to chemical degradation in presence of 45S5 bioglass (Eqtesadi et al., 2016).

All in all, these experimental results highlight the key role of polymer composition on the mechanical reinforcement provided by the deposited layer. In particular, the strengthening and toughening provided by the coating seem to be determined, on the one hand, by the level of infiltration of the scaffold struts' microporosity by the polymer solution and, on the other hand, by the interfacial adhesion between the scaffold material and the polymeric coating. The intrinsic

mechanical performance (stiffness, strength, toughness) of the polymeric material surely plays a role in the reinforcement obtained upon coating. However, the present results seem to suggest that polymer properties are somewhat secondary. That would explain why synthetic polymers such as PLA, which are nominally stronger and stiffer than natural polymers evaluated in this study, do not exhibit an improved performance as reinforcing agents.

Since the interfacial adhesion plays a key role in the enhancement of mechanical properties through polymeric coatings, one effective strategy to improve the mechanical performance would be to produce the coating by *in situ* polymerization (Martínez-Vázquez et al., 2013a): i.e. by immersing the scaffold in a monomeric solution with the appropriate initiators and catalysts. Such coating procedure will induce the formation of a strong bonding between the bioceramic scaffold and the polymeric coating. Moreover, covalently grafting the corresponding polymer's functional group onto the surface of the bioglass would produce chain entanglements that will dramatically enhance the mechanical properties (Joubert et al., 2004; Moon et al., 2008; Yan et al., 2007).

3.3. SBF degradation and surface mineralization of scaffolds

The degradation behavior upon immersion in a SBF solution of 45S5 bioglass scaffolds coated with the analyzed polymers under optimal conditions is compared in Figure 6 with the data for the bare scaffolds obtained in a previous work (Motealleh et al., 2017). This figure shows the evolution of the pH of the SBF solution (Fig. 6a) and the scaffolds' weight loss (Fig. 6b) with immersion time.

Solution pH in the coated structures is simultaneously influenced by degradation of the polymeric coating and dissolution of the bioglass support. The polymeric coatings can

effectively act as a protective layer against degradation of the bioglass substrate upon immersion in the SBF. However, all these polymeric compositions are themselves susceptible to hydrolytic degradation. This results in the release of different organic degradation products which can affect the solution pH. Consequently, the pH differences between the various polymer-coated bioglass scaffolds evidenced in Fig. 6a are not surprising. In any case, with the possible exception of gelatin, all coatings seem to increase the required time to balance the pH values (from 1–2 weeks to up to 8 weeks), and tend to lower the final equilibrium level. This confirms, on the one hand, that bioglass degradation is delayed by polymer coatings leading to a reduction in the ion exchange rate compared to the bare structures. On the other hand, this indicates that the degradation products of all the analyzed polymers are slightly acidic. This is especially true for the synthetic polymers (full symbols), particularly PLA, which yield a more clear pH reduction over the bare scaffolds, while for the natural compositions (open symbols in Fig. 6a) pH values remain closer to those of the bare structure.

The weight loss curves in Fig. 6b reveal an even clearer distinction between the water soluble natural polymers and synthetic ones, which exhibit slower hydrolysis rates (Blaker et al., 2011; Sung et al., 2004). Indeed, synthetic polymer coatings significantly reduce the degradation rate of the scaffolds compared to the bare structures. PCL- and PLA-coated scaffolds shows a similar degradation behavior, although PCL-coated scaffolds clearly degrade at lower rates compared to PLA-coated structures. This can be attributed both to the slower degradation of PCL over PLA (Nair and Laurencin, 2007) and to the fact that PLA's more acidic degradation products may facilitate the dissolution of 45S5 bioglass.

In contrast, bioglass scaffolds coated with natural polymers showed faster weight loss rates not only compared to PCL- or PLA-coated structures but even, in some cases, to the bare

scaffolds. This is not surprising, since natural polymers degrade faster than bioceramics (Mohamed et al., 2014), and although their presence as a coating can delay bioglass dissolution, their own faster degradation significantly contributes to the overall weight loss of the structure.

For example, gelatin-coated scaffolds exhibit faster degradation than the bare scaffolds at least up to 1-2 weeks, and then both rates become similar. The highly hydrophilic nature of this polymer at the incubation temperature of 37 °C (Jones, 2004), along with a potentially increased degradation rate of the bioglass as a result of slightly acidic by-products of gelatin degradation might be responsible for this enhanced biodegradation.

On the other hand, alginate-coated scaffolds show initially slower degradation rates than the bare scaffolds during the first week of immersion, but the rate declines more slowly than in the bare scaffolds and eventually, the weight reduction in the former exceeds that of the bare structures. This is again attributed to the alginate layer dissolution adding to the bioglass degradation. The lower degradation rate exhibited by alginate-coated structures compared to gelatin hybrids is likely due to some degree of cross-linking occurring in the alginate layer induced by the calcium ions in the SBF solution. Crosslinking would indeed enhance the stability of the alginate network and retard its degradation (Draget et al., 2005).

Finally, chitosan-coated scaffolds exhibited the lowest degradation rate among the natural polymer hybrids, and their weight loss remained below the values for the bare structure during the whole immersion period, approaching the behavior of synthetic polymer coatings. The stronger interfacial adhesion between the chitosan coating layer and the bioglass substrate in addition to the lower water-uptake ability of chitosan (Despond et al., 2005)—which retards both the bioglass dissolution and its own degradation—might be responsible for this intermediate behavior.

Regarding the *in vitro* bioactivity, mineralization ability of hybrid scaffolds also depends strongly on the nature of the polymeric coating. Surface morphology evolution with SBF immersion time is shown in the SEM micrographs of Figure 7, for bare (Motealleh et al., 2017) and coated scaffolds. On the one hand, PCL tends to delay the formation of precipitates in the scaffold surfaces. While bare structures show evidence of mineral nucleation even after just one day of immersion (see inset in Fig. 7a), in PCL-coated bioglass scaffolds (Figs. 7d-f) the mineral layer requires more time to nucleate and grow on the rod surface. Initially, depositing crystallites are embedded in the polymer layer (Fig. 7d), implying that the reprecipitation occurs at the bioglass/polymer interface upon diffusion of the appropriate SBF ions through the coating. This is also the case in the PLA-coated scaffolds, although in this sample instance nucleation is already evident after 1 day (Fig. 7g). The aforementioned chemical interactions occurring at the interface between PLA and 45S5 bioglass seem to be facilitating nucleation—PLA acidic degradation products enhance dissolution of the bioglass, producing a local supersaturation of calcium and phosphate ions— as evidenced by the greater number of nuclei observable in Fig. 7g compared to the bare structures (Fig. 7a). This translates also to a greater level of mineralization for longer times (Figs. 7h-i, *vs*. Figs. 7b-c). As the mineralization layer grows, more particles appear on the surface of the rods and eventually microcracks begin to develop in the polymer layer (Figs. 7f, 7h-i). Partial disruption of the coating layer facilitates further SBF penetration into the interface which increases the degradation rate, in good agreement with the results in Fig. 6b, and the growth of the mineralization layer.

On the other hand, bioglass scaffolds coated with natural polymers, especially with chitosan, exhibit a significantly enhanced *in vitro* bioactivity compared not only to synthetic polymer-coated scaffolds but even to the bare structures. All scaffolds coated with natural

polymers show significant amounts of mineralization on their immersion in the SBF (Figs. 7j, 7m, 7p). This is attributed to the hydrophilic nature and high resorption ability of natural polymers in the physiological fluids, and the slightly acidic nature of their degradation products, which can facilitate the solution-reprecipitation process. In this case, nucleation seems to be occurring also directly onto the polymeric coatings rather than just at the interface which can also facilitate the process. This faster nucleation may explain why the weight loss is initially slightly lower in the natural polymer-coated scaffolds (with the exception of gelatin) compared to the bare structures. Mineralization progresses steadily with soaking time until the struts are fully covered by newly formed crystals. Even after 8 weeks, there is still evidence of residual polymers, especially in the case of alginate and chitosan (see insets in Figs. 7l and 7o). Permanence of these polymers in the SBF solution for such a long time is probably attributed to the cross-linking of alginate by calcium ions in the SBF that slows down its dissolution (Draget et al., 2005), and the fact that above pH 6 chitosan becomes insoluble in water (Saïed and Aider, 2014).

Consequently, with the exception of PCL, the application of polymer coatings — especially natural polymers—has a positive effect on the *in vitro* bioactivity of 45S5 bioglass, accelerating the formation of a mineralization layer. And more interestingly, this happens while simultaneously reducing (except in the case of gelatin) the degradation rate of the bioglass scaffold (Fig. 6b). This has a positive impact on the evolution of the scaffold's mechanical properties, as will be discussed in the following section.

On the other hand, the micrographs in Figure 7 show also morphological differences in the mineralization layer deposited onto each coated scaffold. In an attempt to identify the nature of the precipitating phases in each case, XRD spectra were obtained for coated 45S5 bioglass

scaffolds after immersion in the SBF for 8 weeks and compared to similar data for bare scaffolds from previous work (Motealleh et al., 2017) (Figure 8). According to those results, the layer deposited on the surface of the amorphous bare 45S5 bioglass scaffolds after 28 days of immersion in SBF consists of calcite (calcium carbonate, $CaCO_3$) as the main crystalline phase, although evidence of precipitation of amorphous calcium phosphate is also found. Calcite is also the main crystalline phase observed on the surfaces of coated scaffolds after 8 weeks of immersion in the SBF, although sodium calcium silicate ($Na_2CaSi_3O_8$, PDF 00-012-0671)—not an uncommon phase to be found after immersion of 45S5 bioglass in SBF (Porwal et al., 2014)— is also found in the samples coated with natural polymers. Additionally, in the case of chitosan and PLA a few peaks are compatible with the crystallization of apatite crystals. Chitosan-coated samples show also higher peak intensities, which confirms SEM observations of the great level of mineralization occurring in this type of hybrid structures. On the whole, all the deposited phases have been observed also by other authors upon immersion of 45S5 bioglass in the SBF, and none of them are deemed to pose a particular threat to the biological performance of the hybrid scaffolds. Of course, the issue of their respective biological performance would warrant further research. Such a study should be tackled preferably through *in vivo* testing, since cell culture experiments in robocast 45S5 bioglass scaffolds have proven to be highly challenging and tricky (Motealleh et al., 2017).

3.4. Mechanical properties degradation

In the preceding section, , the process of dissolution and reprecipitation occurring in 45S5 bioglass scaffolds before and after coating with different synthetic and natural polymers has been analyzed in detail. However, the question remains as to how these processes affect the

mechanical performance of each type of robocast scaffold. Accordingly, the mechanical degradation of the coated scaffolds with the immersion time in the SBF was evaluated in terms of both compressive strength (Figure 9) and toughness (Figure 10) and compared to data for bare structures from a previous work (Motealleh et al., 2017).

The data in Fig. 9a evidence that the compressive strengths of coated scaffolds are substantially higher than that of the bare structures at all time points tested (Fig. 9a). Chitosan-coated samples show the highest compressive strength at all periods of immersion. Besides, a monotonous decline of the compressive strength with immersion time is observed for all samples. This strength degradation upon immersion in SBF is better analyzed in Fig. 9b, where the compressive strength loss, $\Delta\sigma_C/\sigma_{C0}$, is plotted —with $\Delta\sigma_C = \sigma_{C0}-\sigma_{Ct}$, σ_{C0} being the initial compressive strength of the scaffold, and σ_{Ct} its compressive strength at time t —. From this plot, it is evident that gelatin-coated scaffolds exhibit the fastest degradation and the highest total compression loss (~ 88 ± 2 %). In good accordance with the weight loss results (Fig. 6b), this overall compression loss is even greater than in the bare scaffolds (83 ± 3 %). Alginate-coated scaffolds show a strength loss somewhat similar to the bare structures, with values above or below those of the uncoated scaffolds depending on the immersion period. On the other hand, PCL, PLA and chitosan, in this order, produced the most protective coatings against *in vitro* mechanical degradation, according to compression strength loss measurements. In particular, PCL reduced the total strength loss after 8 weeks of immersion by 13 % over the bare scaffold, although it still remained around 70 %.

Regarding toughness, its evolution in coated scaffolds with the immersion time (Figure 10), elicits very similar comments. The strain energy density values (Fig. 10a) are enhanced by all polymer coatings, and at all time-points, even more significantly than in the case of strength.

Thus, even the faster-degrading gelatin and alginate hybrid structures (Fig. 6b) remain around an order of magnitude tougher than the bare scaffolds over the whole degradation period time. This result confirms the presence of residual polymers in the scaffold even after 8 weeks of immersion in SBF, in good agreement with SEM observations (Fig. 7).

The evolution of toughness loss (Fig. 10b)—defined as $\Delta G_C/G_{C0,}$ with $\Delta G_C = G_{C0} - G_{Ct}$, G_{C0} and G_{Ct} the toughness of the scaffold before and after immersion for a time t— suggests that toughness degradation is initially less abrupt than strength loss (Fig. 9b), especially in bare and gelatin- and alginate-coated scaffolds. As a consequence, the differences between the various systems are reduced. Although the synthetic polymers, followed by chitosan, remain the most effective coating materials for delaying the degradation of the mechanical performance of 45S5 bioglass scaffolds.

4. Implications

This study has demonstrated that dip-coating of robocast structures with either natural or synthetic commercial polymers can be used as a simple, cost-effective technique for the preparation of organic/inorganic hybrid scaffolds in a reliable way. The deposited polymers penetrate the struts' microporosity while preserving the pre-designed interconnected macropore architecture of robocast scaffolds intact. The compressive strength and toughness of amorphous 45S5 bioglass bare scaffolds was significantly enhanced by coating with any of the investigated polymers. With a careful selection of the biodegradable polymeric coating, it is possible to fabricate hybrid scaffolds with mechanical performance comparable to that of cancellous bone in compression: i.e. with clearly superior strength and toughness within the lower limit of trabecular bone values (Figure 11).

Polymer composition plays a key role in the mechanical reinforcement provided by the deposited coating. The results obtained in this work evidence that 45S5 bioglass scaffolds coated with natural polymers (gelatin, alginate an chitosan) exhibit higher strength and toughness than those coated with synthetic ones (PCL and PLA), despite the *a priori* superior intrinsic mechanical properties of the latter. This result suggests that the level of impregnation and the interfacial adhesion—most likely stronger between the similarly hydrophilic bioglass and natural polymers than between the former and the more hydrophobic synthetic compositions—plays a major role in the mechanical reinforcement produced by the polymeric coating. Thus, the intrinsic properties (stiffness, strength, and toughness) of the polymer apparently remain a secondary factor, at least for the systems studied here.

While all this mechanical enhancement can come, as in the case of PCL, at the cost of reducing the bioactivity of the 45S5 bioglass scaffold, most of the analyzed polymers yielded hybrid structures with enhanced mineralization *in vitro*. The presence of the polymer has an additional benefit, as it provides a means for tailoring the degradation behavior of 45S5 bioglass scaffolds. Polymeric coatings provide, with the sole exception of gelatin, a suitable barrier against the degradation of the bioglass substrate, and its mechanical performance, in physiological environment. In this sense, synthetic polymers offer the most effective protection against degradation, followed closely by chitosan.

As a final remark, it is worth highlighting that among all synthetic and natural polymers analyzed in this study, chitosan outstands as the optimal coating material for the mechanical and biological enhancement of 45S5 bioglass robocast scaffolds. This natural polymer not only provides superior initial toughening and strengthening, but also lessens mechanical degradation

nearly as much as the less biodegradable synthetic polymers. And all that while simultaneously enhancing the *in vitro* bioactivity of 45S5 bioglass robocast scaffolds.

Acknowledgements

The authors want to acknowledge the aid of Dr. Angel Luis Ortiz in the analysis of XRD data. Funding: This work was supported by the European Union Seventh Framework Programme [grant number 604036], by the Ministerio de Economía y Competitividad [grant MAT2015-64670-R (MINECO/FEDER)], by the Gobierno de Extremadura [grant IB13007] and the Fondo Europeo de Desarrollo Regional (FEDER).

References

Al-Sagheer, F., Muslim, S., 2010. Thermal and mechanical properties of chitosan/SiO2 hybrid composites. J. Nanomater. 2010, 1–7. doi:10.1155/2010/490679

Allo, B.A., Rizkalla, A.S., Mequanint, K., 2010. Synthesis and electrospinning of ε-polycaprolactone-bioactive glass hybrid biomaterials via a sol-gel process. Langmuir 26, 18340–8. doi:10.1021/la102845k

Blaker, J.J., Nazhat, S.N., Maquet, V., Boccaccini, A.R., 2011. Long-term in vitro degradation of PDLLA/Bioglass® bone scaffolds in acellular simulated body fluid. Acta Biomater. 7, 829–840. doi:10.1016/j.actbio.2010.09.013

Bretcanu, O., Chen, Q., Misra, S.K., Boccaccini, A.R., Roy, I., Verne, E., Brovarone, C.V., 2007. Biodegradable polymer coated 45S5 Bioglass-derived glass-ceramic scaffolds for bone tissue engineering. Glas. Technol. Eur. J. Glas. Sci. Technol. Part A 48, 227–234.

Cesarano, J., Segalman, R., Calvert, P., 1998. Robocasting provides moldless fabrication from slurry deposition. Ceram. Ind. 148, 94–102.

Cesarano III, Joseph; calvert, D.P., 2000. Freeforming Objects With low Binder Slurry. United States Pat.

Chen, Q.Z., Ahmed, I., Knowles, J.C., Nazhat, S.N., Boccaccini, A.R., Rezwan, K., 2008. Collagen release kinetics of surface functionalized 45S5 Bioglass®-based porous scaffolds. J. Biomed. Mater. Res. - Part A 86, 987–995. doi:10.1002/jbm.a.31718

Chen, Q.Z., Boccaccini, A.R., 2006. Poly(D,L-lactic acid) coated 45S5 Bioglass®-based scaffolds: Processing and characterization. J. Biomed. Mater. Res. - Part A 77, 445–457. doi:10.1002/jbm.a.30636

Despond, S., Espuche, E., Cartier, N., Domard, A., 2005. Hydration mechanism of polysaccharides: A comparative study. J. Polym. Sci. Part B Polym. Phys. 43, 48–58. doi:10.1002/polb.20277

Draget, K.I., Smidsrød, O., Skjåk-Bræk, G., 2005. Alginates from algae, in: Steinbuchel, A., Rhee, S.K. (Eds.), Polysaccharides and Polyamides in the Food Industry. Wiley-VCH-Verlag, pp. 1–30. doi:10.1002/3527600035.bpol6008

Eqtesadi, S., Motealleh, A., Miranda, P., Lemos, A., Rebelo, A., Ferreira, J.M.F., 2013a. A simple recipe for direct writing complex 45S5 Bioglass® 3D scaffolds. Mater. Lett. 93, 68–71. doi:10.1016/j.matlet.2012.11.043

Eqtesadi, S., Motealleh, A., Miranda, P., Lemos, A., Rebelo, A., Ferreira, J.M.F., 2013b. A simple recipe for direct writing complex 45S5 Bioglass®3D scaffolds. Mater. Lett. 93, 68–71. doi:10.1016/j.matlet.2012.11.043

Eqtesadi, S., Motealleh, A., Miranda, P., Pajares, A., Lemos, A., Ferreira, J.M.F., 2014. Robocasting of 45S5 bioactive glass scaffolds for bone tissue engineering. J. Eur. Ceram. Soc. 34, 107–118. doi:10.1016/j.jeurceramsoc.2013.08.003

Eqtesadi, S., Motealleh, A., Pajares, A., Guiberteau, F., Miranda, P., 2015. Influence of sintering temperature on the mechanical properties of □-PCL-impregnated 45S5 bioglass-derived scaffolds fabricated by robocasting. J. Eur. Ceram. Soc. 35, 3985–3993. doi:10.1016/j.jeurceramsoc.2015.06.021

Eqtesadi, S., Motealleh, A., Perera, F.H., Pajares, A., Miranda, P., 2016. Poly-(lactic acid) infiltration of 45S5 Bioglass® robocast scaffolds: Chemical interaction and its deleterious effect in mechanical enhancement. Mater. Lett. 163, 196–200. doi:10.1016/j.matlet.2015.10.073

Erol, M.M., Mouriño, V., Newby, P., Chatzistavrou, X., Roether, J.A., Hupa, L., Boccaccini, A.R., 2012. Copper-releasing, boron-containing bioactive glass-based scaffolds coated with alginate for bone tissue engineering. Acta Biomater. 8, 792–801. doi:10.1016/j.actbio.2011.10.013

Gerhardt, L.-C., Boccaccini, A.R., 2010. Bioactive Glass and Glass-Ceramic Scaffolds for Bone Tissue Engineering. Materials (Basel). doi:10.3390/ma3073867

Govindan, R., Kumar, G.S., Girija, E.K., 2015. Polymer coated phosphate glass/hydroxyapatite composite scaffolds for bone tissue engineering applications. RSC Adv. 5, 60188–60198. doi:10.1039/C5RA09258B

Jones, B.E., 2004. Manufacture and Properties of Two-piece Hard Capsules, in: Podczeck, F., Jones, B.E. (Eds.), Pharmaceutical Capsules. Pharmaceutical Press, p. 95.

Jones, J.R., 2013. Review of bioactive glass: From Hench to hybrids. Acta Biomater. doi:10.1016/j.actbio.2012.08.023

Joubert, M., Delaite, C., Bourgeat-Lami, E., Dumas, P., 2004. Ring-Opening polymerization of ε-Caprolactone and L-Lactide from silica nanoparticles surface. J. Polym. Sci. Part A Polym. Chem. 42, 1976–1984. doi:10.1002/pola.20035

Keller, T.S., Mao, Z., Spengler, D.M., 1990. Young's modulus, bending strength, and tissue physical properties of human compact bone. J. Orthop. Res. 8, 592–603. doi:10.1002/jor.1100080416

Kokubo, T., Takadama, H., 2006. How useful is SBF in predicting in vivo bone bioactivity? Biomaterials 27, 2907–2915. doi:10.1016/j.biomaterials.2006.01.017

Li, J.J., Gil, E.S., Hayden, R.S., Li, C., Roohani-Esfahani, S.I., Kaplan, D.L., Zreiqat, H., 2013. Multiple silk coatings on biphasic calcium phosphate scaffolds: Effect on physical and mechanical properties and in vitro osteogenic response of human mesenchymal stem cells. Biomacromolecules 14, 2179–2188. doi:10.1021/bm400303w

Li, W., Ding, Y., Rai, R., Roether, J.A., Schubert, D.W., Boccaccini, A.R., 2014a. Preparation

and characterization of PHBV microsphere/45S5 bioactive glass composite scaffolds with vancomycin releasing function. Mater. Sci. Eng. C 41, 320–328. doi:10.1016/j.msec.2014.04.052
Li, W., Garmendia, N., Perez de Larraya, U., Ding, Y., Detsch, R., Gruenewald, A., Roether, J., Schubert, D., Boccaccini, A.R., 2014b. 45S5 bioactive glass-based scaffolds coated with cellulose nanowhiskers for bone tissue engineering. RSC Adv. 4, 56156–56164.
Martínez-Vázquez, F.J., Miranda, P., Guiberteau, F., Pajares, A., 2013a. Reinforcing bioceramic scaffolds with in situ synthesized ε-polycaprolactone coatings. J. Biomed. Mater. Res. - Part A 101, 3551–3559. doi:10.1002/jbm.a.34657
Martínez-Vázquez, F.J., Pajares, A., Guiberteau, F., Miranda, P., 2014. Effect of polymer infiltration on the flexural behavior of β-tricalcium phosphate robocast scaffolds. Materials (Basel). 7, 4001–4018. doi:10.3390/ma7054001
Martínez-Vázquez, F.J., Perera, F.H., Meulen, I. Van Der, Heise, A., Pajares, A., Miranda, P., 2013b. Impregnation of β-tricalcium phosphate robocast scaffolds by in situ polymerization. J. Biomed. Mater. Res. - Part A 101, 3086–3096. doi:10.1002/jbm.a.34609
Martínez-Vázquez, F.J., Perera, F.H., Miranda, P., Pajares, A., Guiberteau, F., 2010. Improving the compressive strength of bioceramic robocast scaffolds by polymer infiltration. Acta Biomater. 6, 4361–4368. doi:10.1016/j.actbio.2010.05.024
Metze, A.L., Grimm, A., Nooeaid, P., Roether, J.A., Hum, J., Newby, P.J., Schubert, D.W., Boccaccini, A.R., 2013. Gelatin Coated 45S5 Bioglass®-Derived Scaffolds for Bone Tissue Engineering. Key Eng. Mater. 541, 31–39.
Miranda, P., Saiz, E., Gryn, K., Tomsia, A.P., 2006. Sintering and robocasting of β-tricalcium phosphate scaffolds for orthopaedic applications. Acta Biomater. 2, 457–466. doi:10.1016/j.actbio.2006.02.004
Mohamed, K.R., Beherei, H.H., El-Rashidy, Z.M., 2014. In vitro study of nano-hydroxyapatite/chitosan-gelatin composites for bio-applications. J. Adv. Res. 5, 201–8. doi:10.1016/j.jare.2013.02.004
Moon, J.-H., Ramaraj, B., Lee, S.M., Yoon, K.R., 2008. Direct grafting of □-caprolactone on solid core/mesoporous shell silica spheres by surface-initiated ring-opening polymerization. J. Appl. Polym. Sci. 107, 2689–2694. doi:10.1002/app.27369
Motealleh, A., Eqtesadi, S., Civantos, A., Pajares, A., Miranda, P., 2017. Robocast 45S5 bioglass scaffolds: in vitro behavior. J. Mater. Sci. 52, 9179–9191. doi:10.1007/s10853-017-0775-5
Motealleh, A., Eqtesadi, S., Perera, F.H., Pajares, A., Guiberteau, F., Miranda, P., 2016. Understanding the role of dip-coating process parameters in the mechanical performance of polymer-coated bioglass robocast scaffolds. J. Mech. Behav. Biomed. Mater. 64, 253–261. doi:10.1016/j.jmbbm.2016.08.004
Nair, L.S., Laurencin, C.T., 2007. Biodegradable polymers as biomaterials. Prog. Polym. Sci. 32, 762–798. doi:10.1016/j.progpolymsci.2007.05.017
Oudadesse, H., Bui, X.-V., Gal, Y. Le, Mostafa, A., Cathelineau, G., 2011. Chitosan effects on bioactive glass for application as biocopmosite biomaterial. Int. J. Biol. Biomed. Eng. 5, 49–56.
Peroglio, M., Gremillard, L., Chevalier, J., Chazeau, L., Gauthier, C., Hamaide, T., 2007. Toughening of bio-ceramics scaffolds by polymer coating. J. Eur. Ceram. Soc. 27, 2679–2685. doi:10.1016/j.jeurceramsoc.2006.10.016
Philippart, A., Boccaccini, A.R., Fleck, C., Schubert, D.W., Roether, J.A., 2015. Toughening and functionalization of bioactive ceramic and glass bone scaffolds by biopolymer coatings and

infiltration: a review of the last 5 years. Expert Rev. Med. Devices 12, 93–111. doi:10.1586/17434440.2015.958075
Porwal, H., Grasso, S., Cordero-Arias, L., Li, C., Boccaccini, A.R., Reece, M.J., 2014. Processing and bioactivity of 45S5 Bioglass®-graphene nanoplatelets composites. J. Mater. Sci. Mater. Med. 25, 1403–1413. doi:10.1007/s10856-014-5172-x
Rashidova, S.S., Shakarova, D.S., Ruzimuradov, O.N., Satubaldieva, D.T., Zalyalieva, S.V., Shpigun, O.A., Varlamov, V.P., Kabulov, B.D., 2004. Bionanocompositional chitosan-silica sorbent for liquid chromatography. J. Chromatogr. B 800, 49–53. doi:10.1016/j.jchromb.2003.10.015
Roether, J. a., Boccaccini, a. R., Hench, L.L., Maquet, V., Gautier, S., Jérôme, R., 2002. Development and in vitro characterisation of novel bioresorbable and bioactive composite materials based on polylactide foams and Bioglass® for tissue engineering applications. Biomaterials 23, 3871–3878. doi:10.1016/S0142-9612(02)00131-X
Saïed, N., Aider, M., 2014. Zeta potential and turbidimetry analyzes for the evaluation of chitosan/phytic acid complex formation. J. Food Res. 3, 71–81. doi:10.5539/jfr.v3n2p71
Sung, H.-J., Meredith, C., Johnson, C., Galis, Z.S., 2004. The effect of scaffold degradation rate on three-dimensional cell growth and angiogenesis. Biomaterials 25, 5735–5742. doi:10.1016/j.biomaterials.2004.01.066
Wu, C., Zhang, Y., Zhu, Y., Friis, T., Xiao, Y., 2010. Structure-property relationships of silk-modified mesoporous bioglass scaffolds. Biomaterials 31, 3429–3438. doi:10.1016/j.biomaterials.2010.01.061
Yan, S., Yin, J., Yang, Y., Dai, Z., Ma, J., Chen, X., 2007. Surface-grafted silica linked with l-lactic acid oligomer: A novel nanofiller to improve the performance of biodegradable poly(l-lactide). Polymer (Guildf). 48, 1688–1694. doi:10.1016/j.polymer.2007.01.037
Yang, G., Yang, X., Zhang, L., Lin, M., Sun, X., Chen, X., Gou, Z., 2012. Counterionic biopolymers-reinforced bioactive glass scaffolds with improved mechanical properties in wet state. Mater. Lett. 75, 80–83. doi:10.1016/j.matlet.2012.01.122

Figure captions

Figure 1. Schematic diagrams of the fabrication techniques used in this study: (a) robocasting and (b) dip-coating.

Figure 2. Low magnification SEM micrographs of a 45S5 bioglass scaffold after coating with chitosan.

Figure 3. SEM micrographs of the rod surfaces of amorphous 45S5 bioglass scaffolds: before (a) and after coating with alginate (b), chitosan (c), gelatin (d), PCL (e) and PLA (f).

Figure 0. Fracture surfaces of amorphous 45S5 bioglass scaffolds: before (a) and after coating with alginate (b), chitosan (c), gelatin (d), PCL (e) and PLA (f).

Figure 5. Compressive strength (a) and strain energy density at 20 % strain (b) of 45S5 bioglass scaffolds bare (Eqtesadi et al., 2015) and coated with polymers at optimal concentrations: 5 % w/v for alginate (Alg), chitosan (Chi) and gelatin (Gel); 25 % w/v for PCL (Eqtesadi et al., 2015) and 15 % w/v for PLA (Eqtesadi et al., 2016). Patterned bars for PCL and PLA indicate values obtained when using the same concentration as for the natural polymers (5 % w/v).

Figure 6. Evolution of (a) pH of the SBF solution and (b) scaffold's weight loss as a function of immersion time for amorphous 45S5 bioglass scaffolds before and after coating with the indicated polymers, with standard deviations as error bars.

Figure 7. SEM micrographs of the strut surfaces of amorphous 45S5 bioglass scaffolds coated with the indicated polymers after soaking in SBF for the indicated times.

Figure 8. XRD patterns for bare (Motealleh et al., 2017) and polymer-coated 45S5 bioglass samples after immersion in SBF for 8 weeks. Main peaks of the identified crystalline phases are labeled with symbols according to the legend.

Figure 9. Compressive strength (a) and compressive strength loss (b) as a function of immersion time in SBF for bare (Motealleh et al., 2017) and coated 45S5 bioglass scaffolds, with standard deviation as error bars.

Figure 10. Strain energy density at 20 % strain, G_C, (a) and strain energy density loss (b) as a function of immersion time in SBF for bare (Motealleh et al., 2017) and coated 45S5 bioglass scaffolds, with standard deviation as error bars.

Figure 11. Plots of compressive strength, σ_C, versus strain energy density, G_C, for the 45S5 bioglass robocast scaffolds evaluated in this study. Results are compared to cancellous bone properties (Keller et al., 1990).

a)

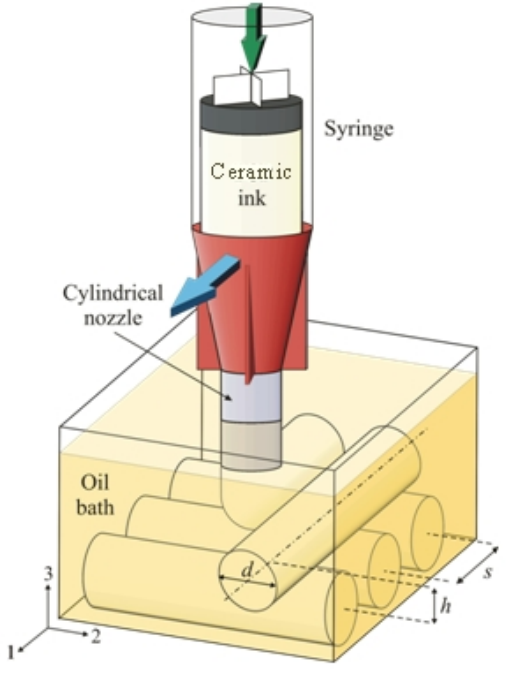

b)

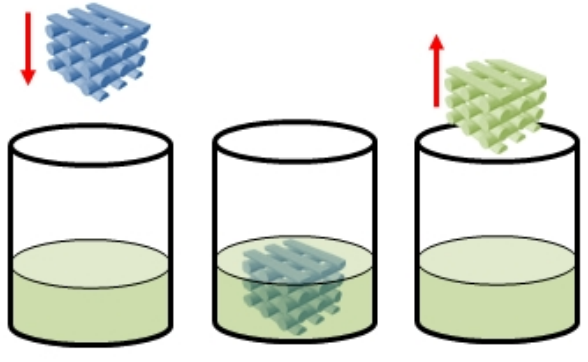

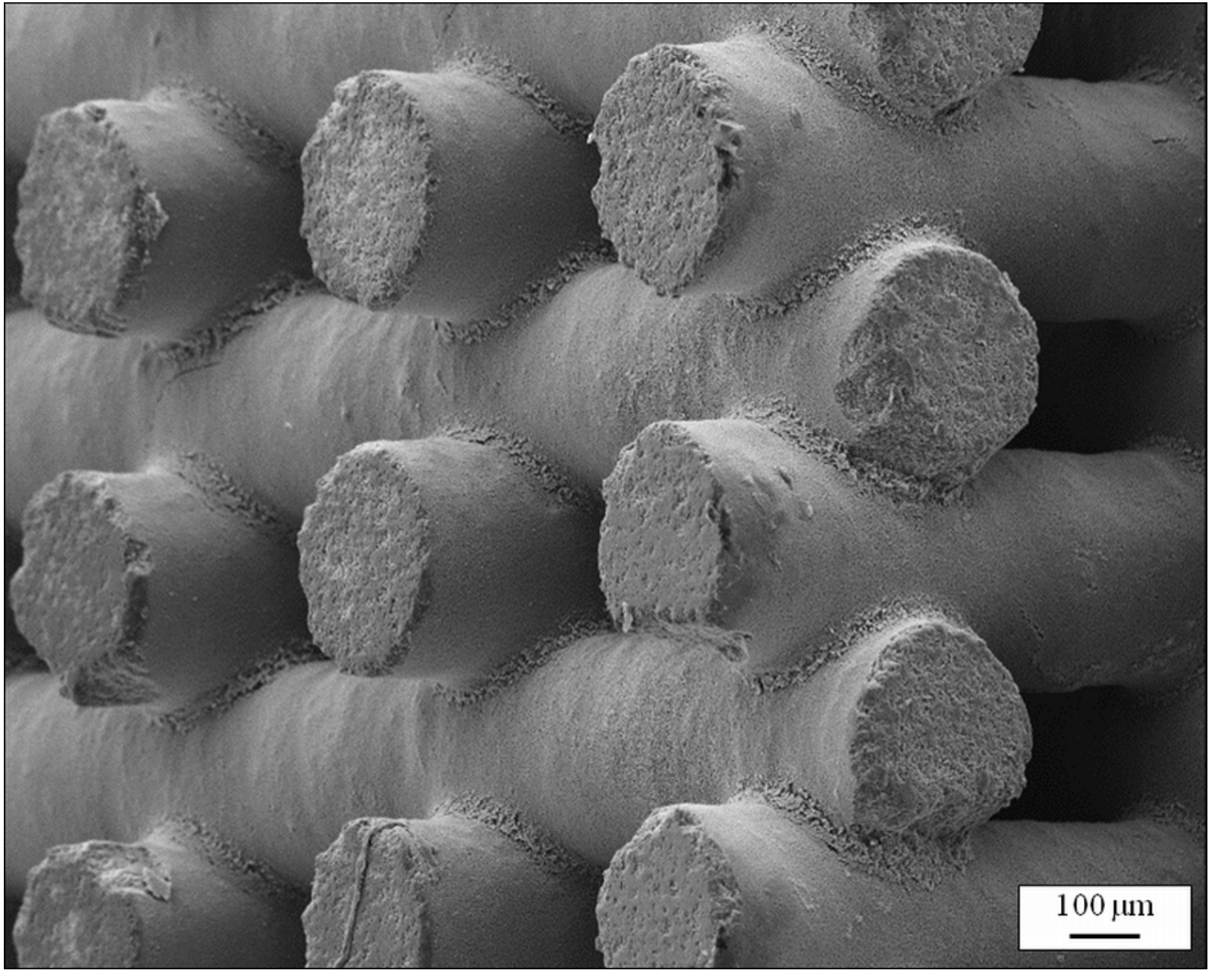
100 µm

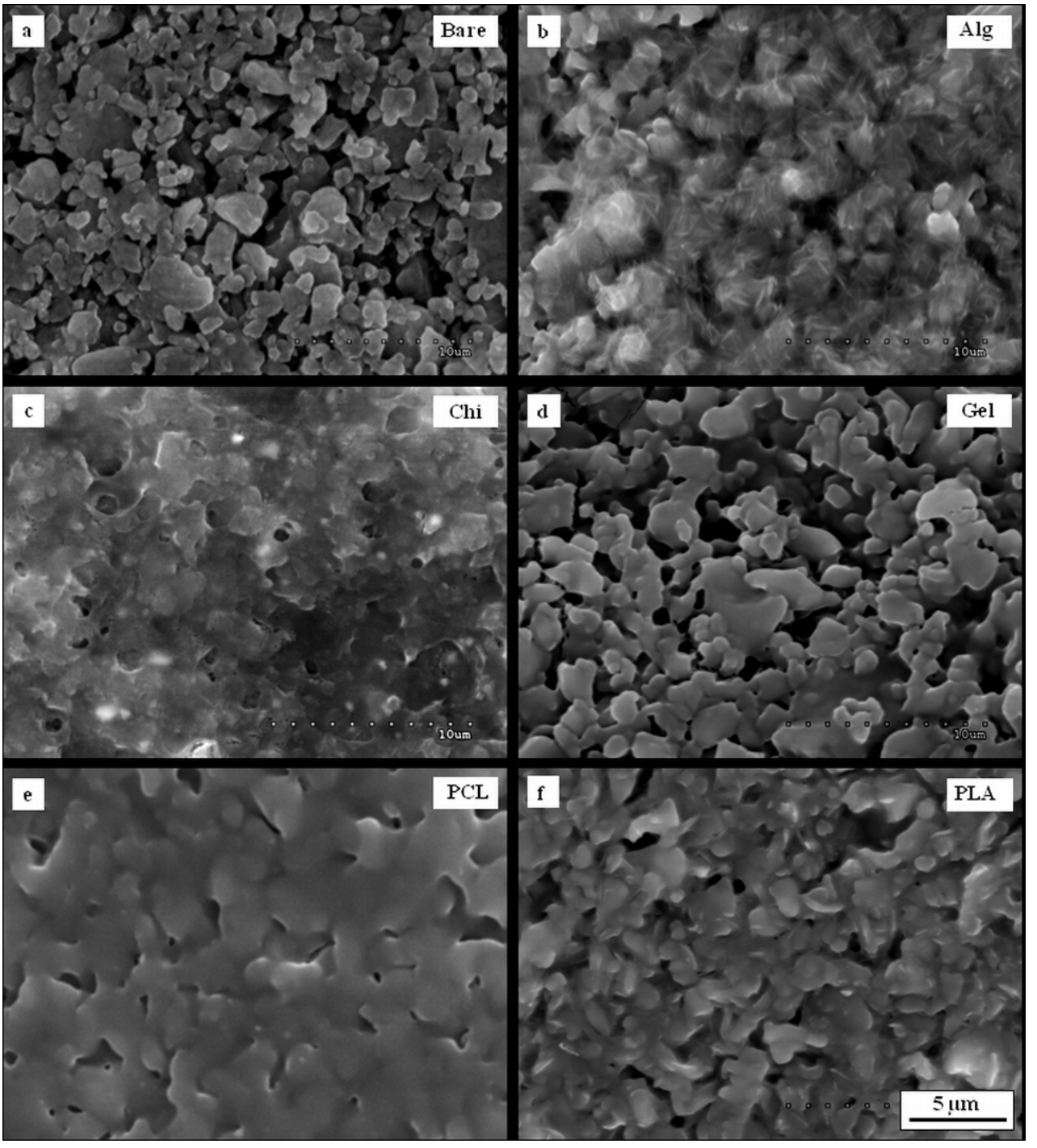
a
Bare
10um
b
Alg
10um
c
Chi
10um
d
Gel
10um
e
PCL
f
PLA
5 µm

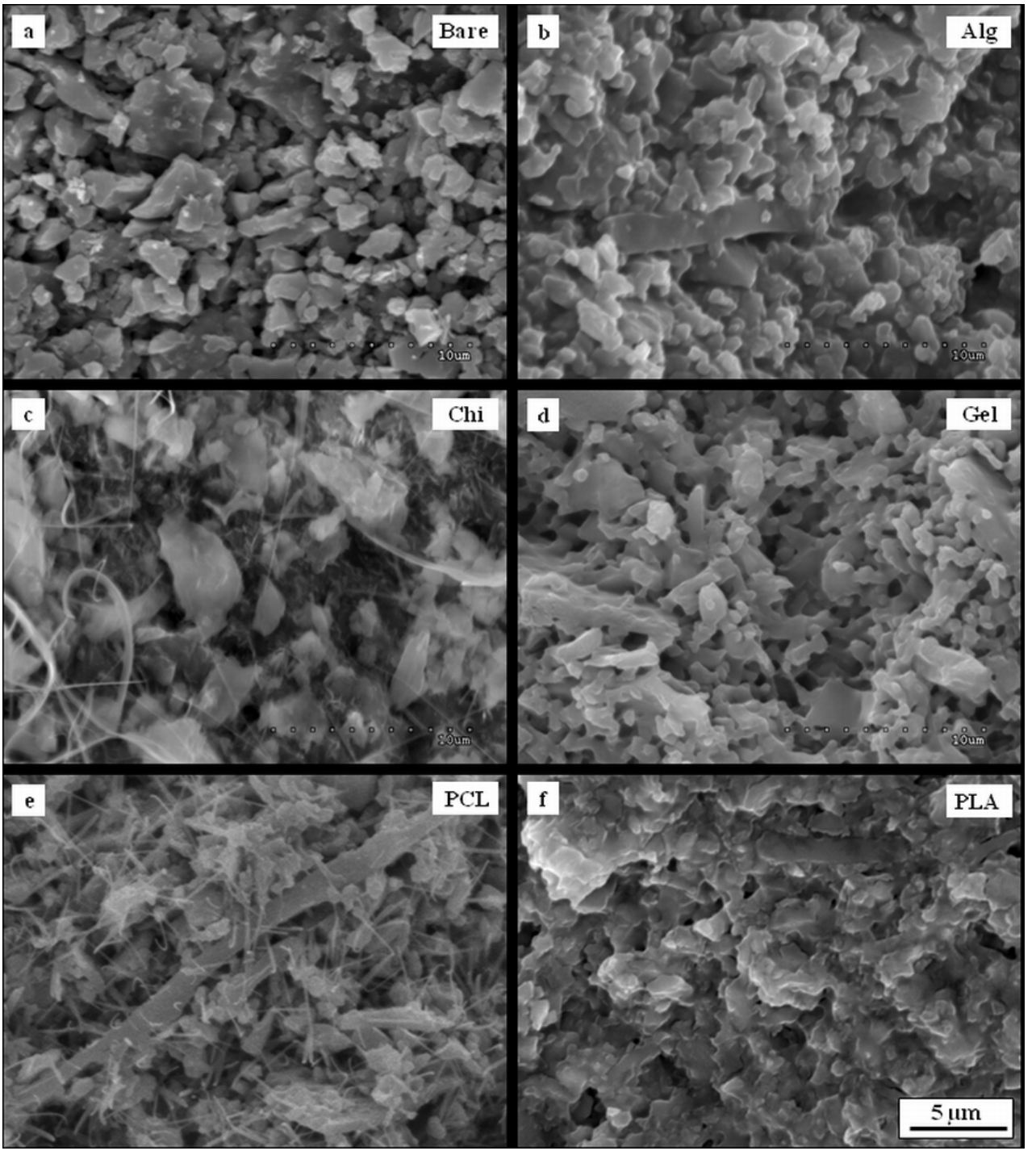
a
Bare
10um
b
Alg
10um
c
Chi
10um
d
Gel
10um
e
PCL
f
PLA
5 µm

a)

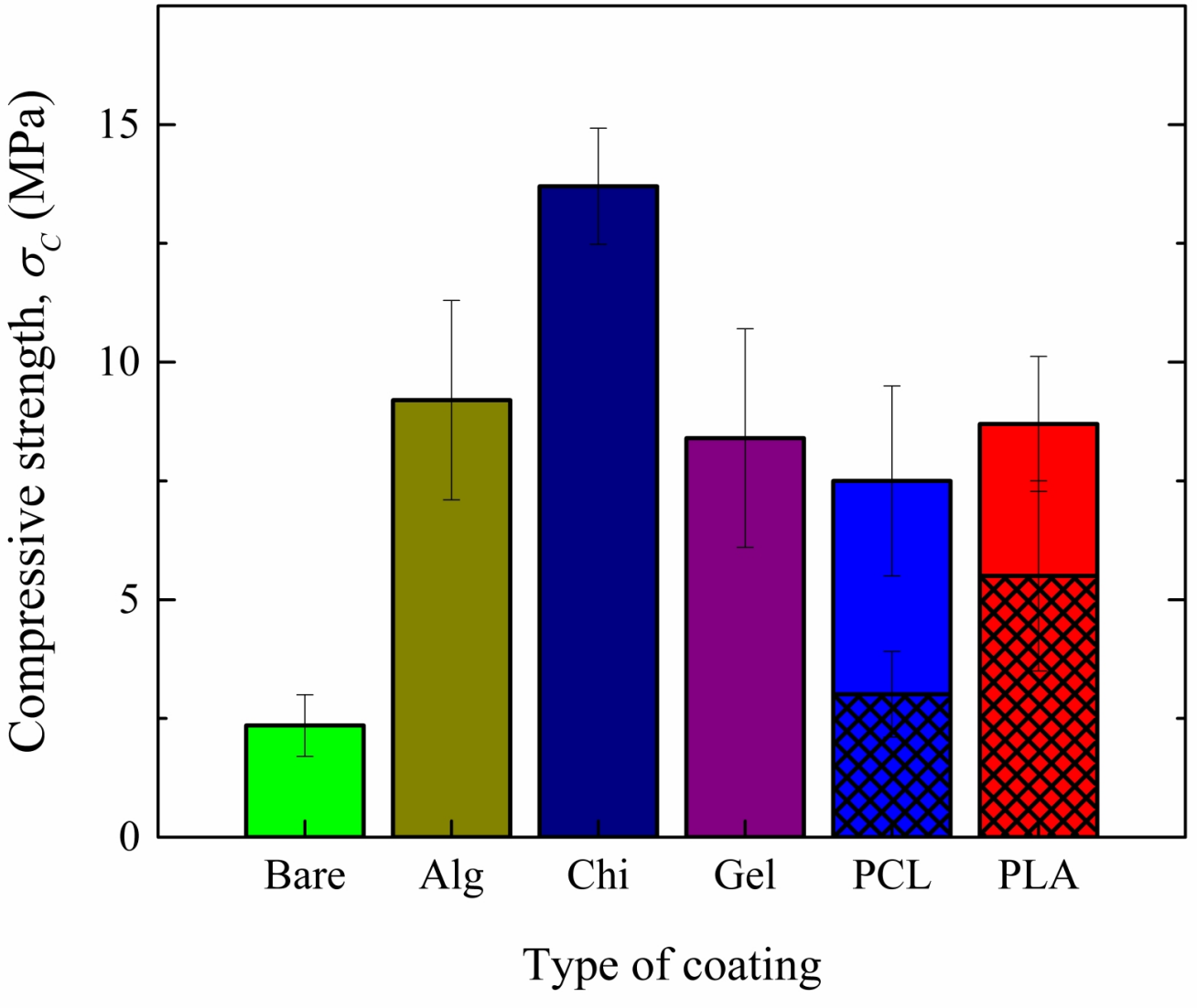
Compressive strength, σ_C (MPa)
0
5
10
15
Bare
Alg
Chi
Gel
PCL
PLA
Type of coating

b)

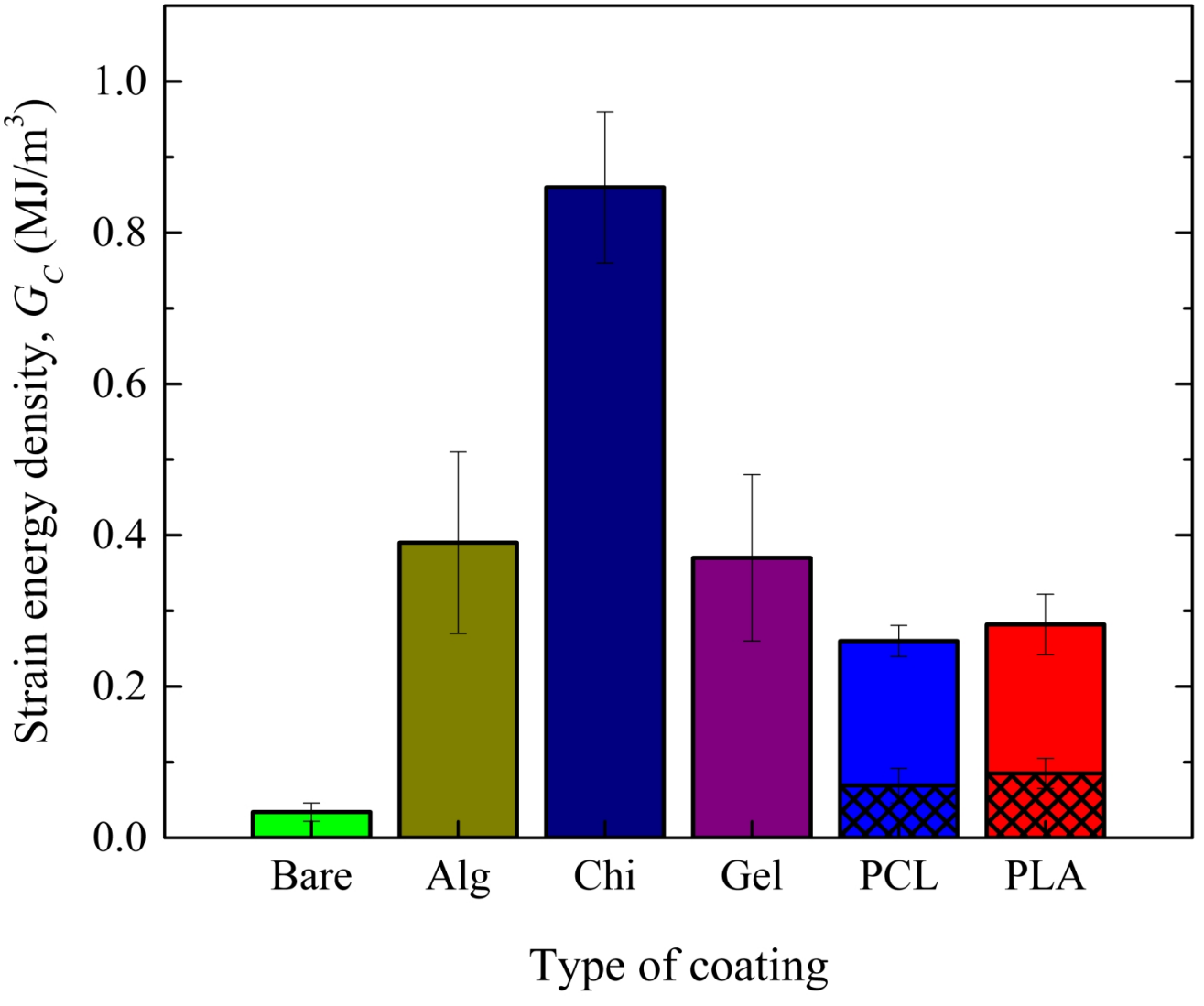
Strain energy density, G_C (MJ/m^3)
1.0
0.8
0.6
0.4
0.2
0.0
Bare
Alg
Chi
Gel
PCL
PLA
Type of coating

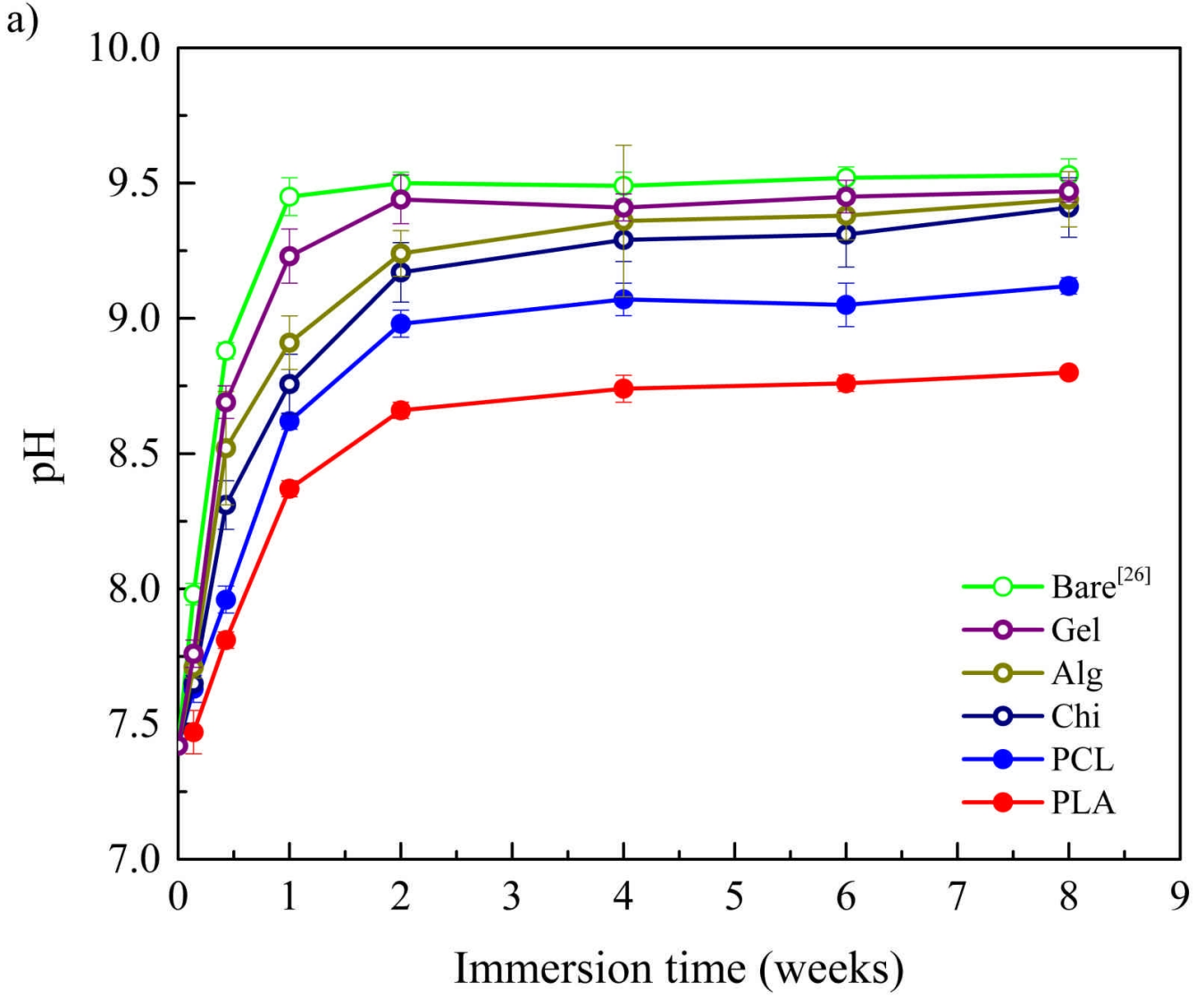
a)
10.0
9.5
9.0
8.5
8.0
7.5
7.0
pH
0
1
2
3
4
5
6
7
8
9
Immersion time (weeks)
Bare[26]
Gel
Alg
Chi
PCL
PLA

b)

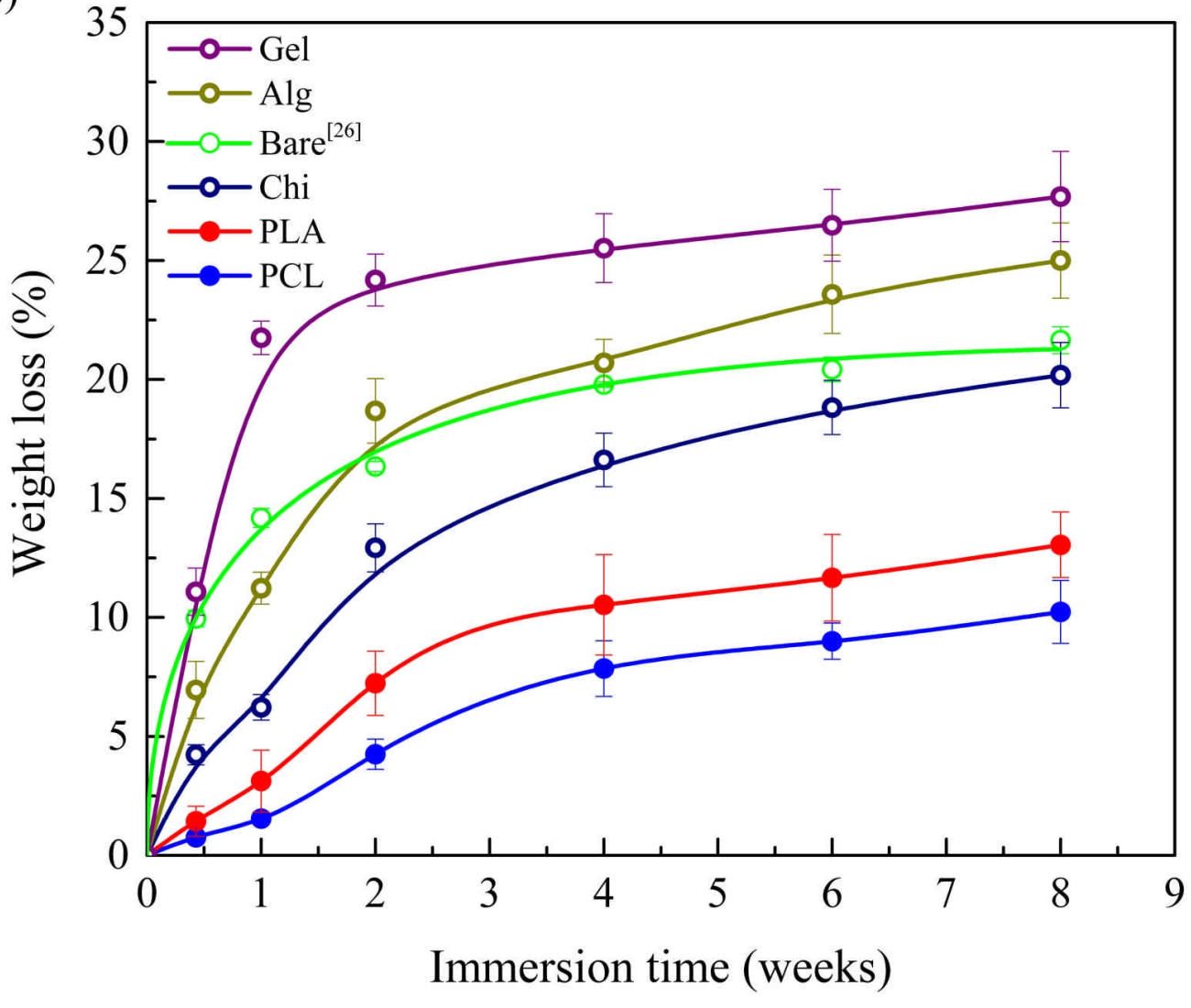
Gel
Alg
Bare[26]
Chi
PLA
PCL
Weight loss (%)
Immersion time (weeks)
0
5
10
15
20
25
30
35
0
1
2
3
4
5
6
7
8
9

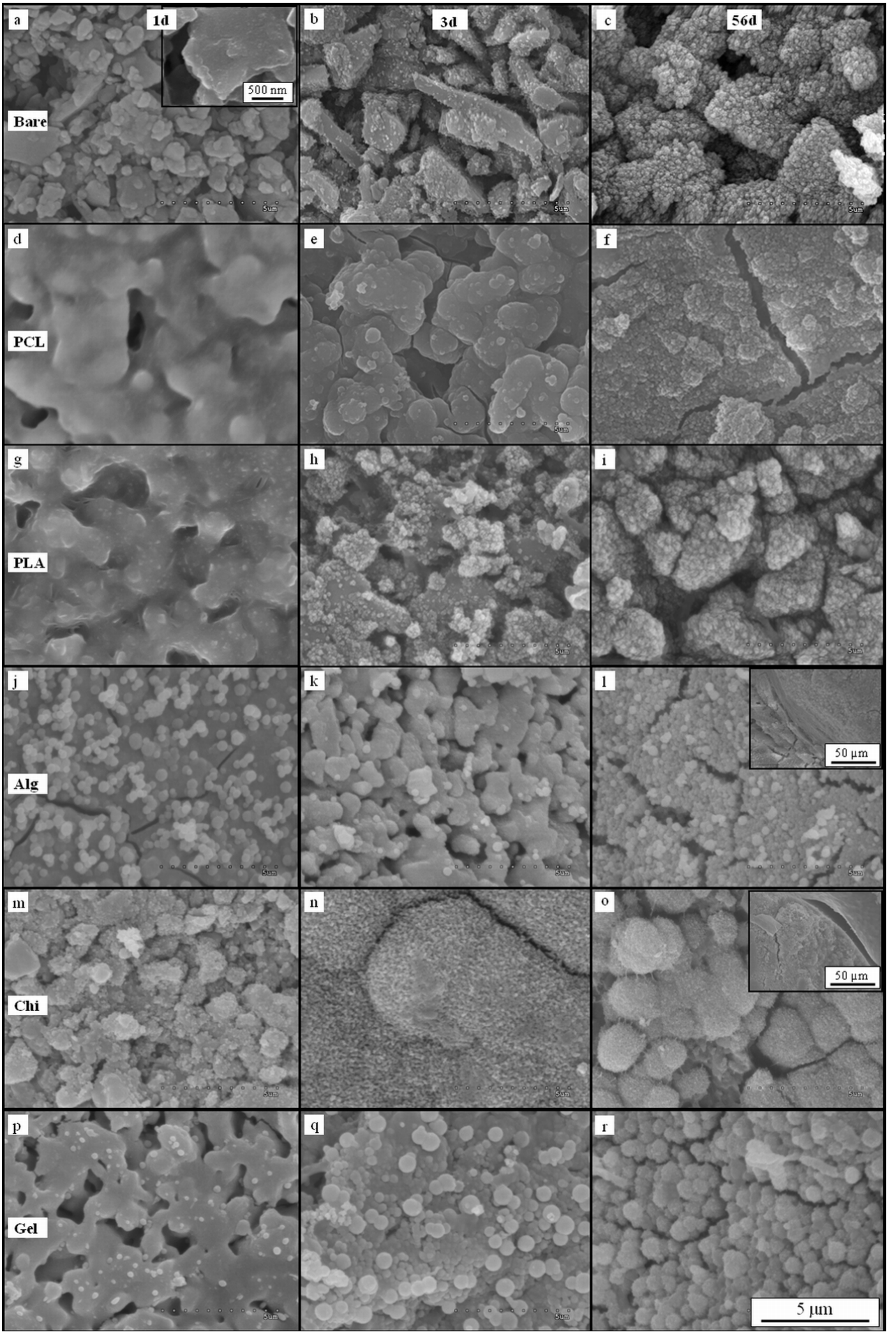
a
1d
500 nm
Bare
b
3d
c
56d
d
PCL
e
f
g
PLA
h
i
j
Alg
k
l
50 µm
m
Chi
n
o
50 µm
p
Gel
q
r
5 µm

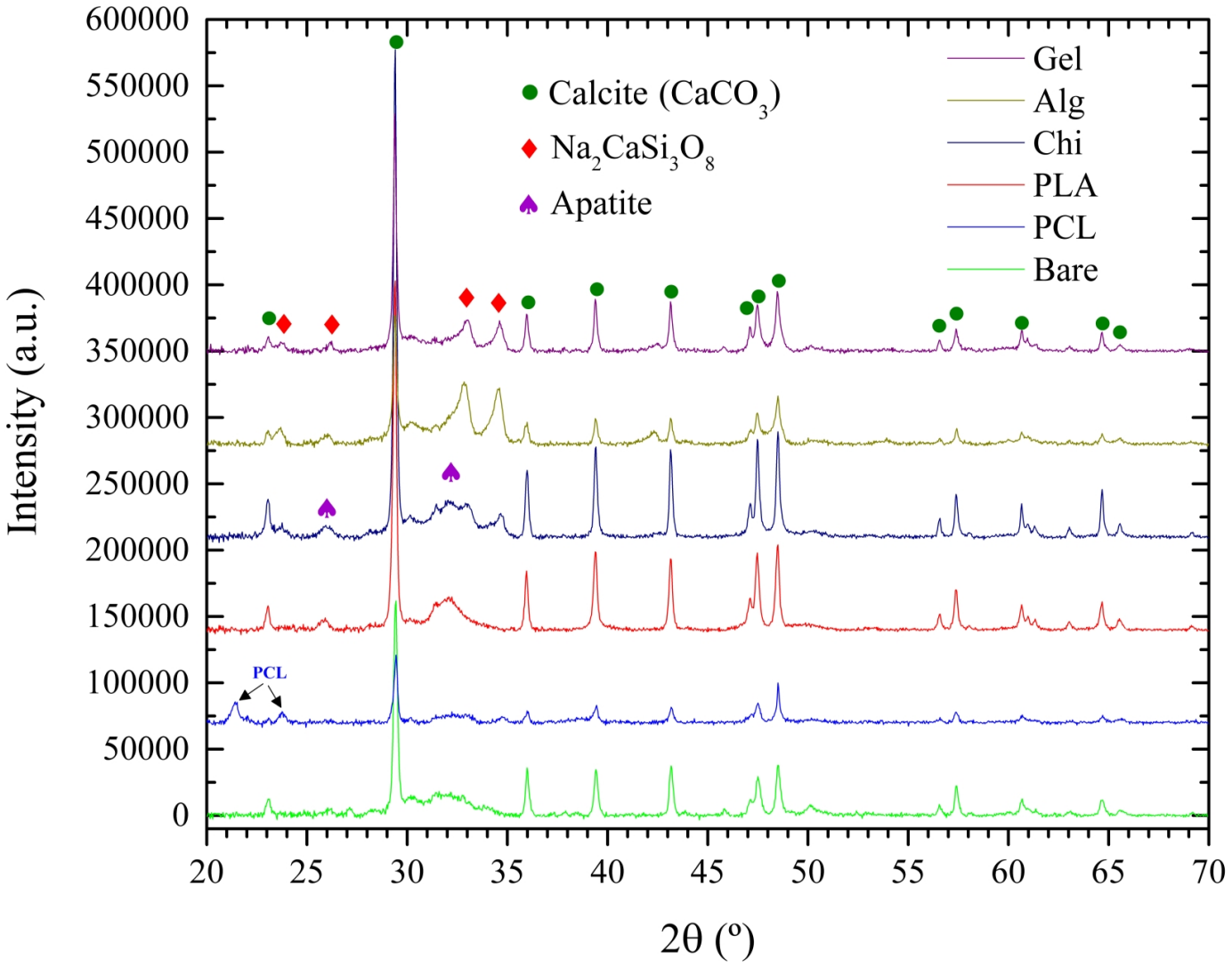
Intensity (a.u.)
600000
550000
500000
450000
400000
350000
300000
250000
200000
150000
100000
50000
0
20
25
30
35
40
45
50
55
60
65
70
2θ (º)
Calcite (CaCO3)
Na2CaSi3O8
Apatite
Gel
Alg
Chi
PLA
PCL
Bare
PCL

a)

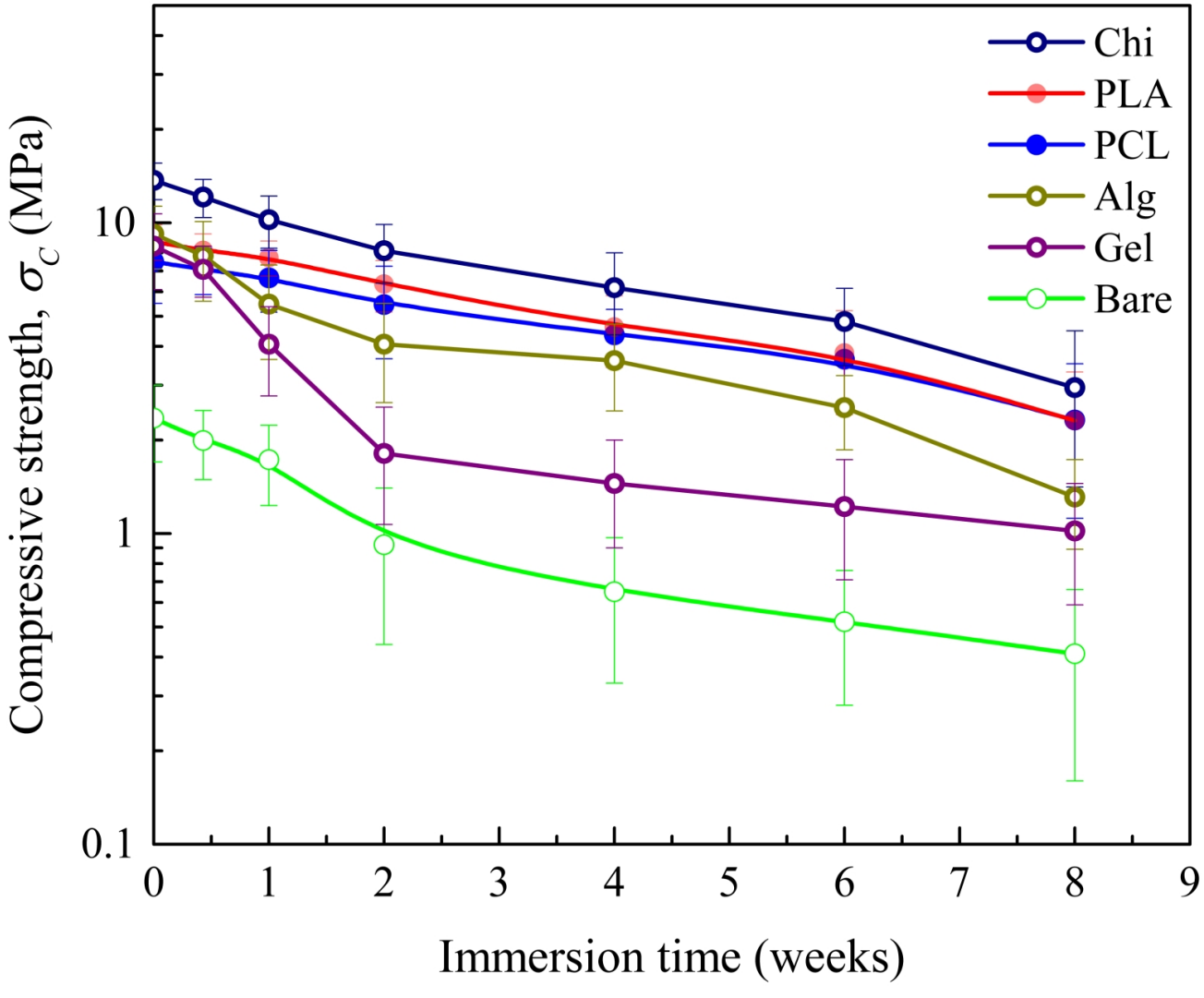
Chi
PLA
PCL
Alg
Gel
Bare
Compressive strength, σ_C (MPa)
10
1
0.1
0
1
2
3
4
5
6
7
8
9
Immersion time (weeks)

b)

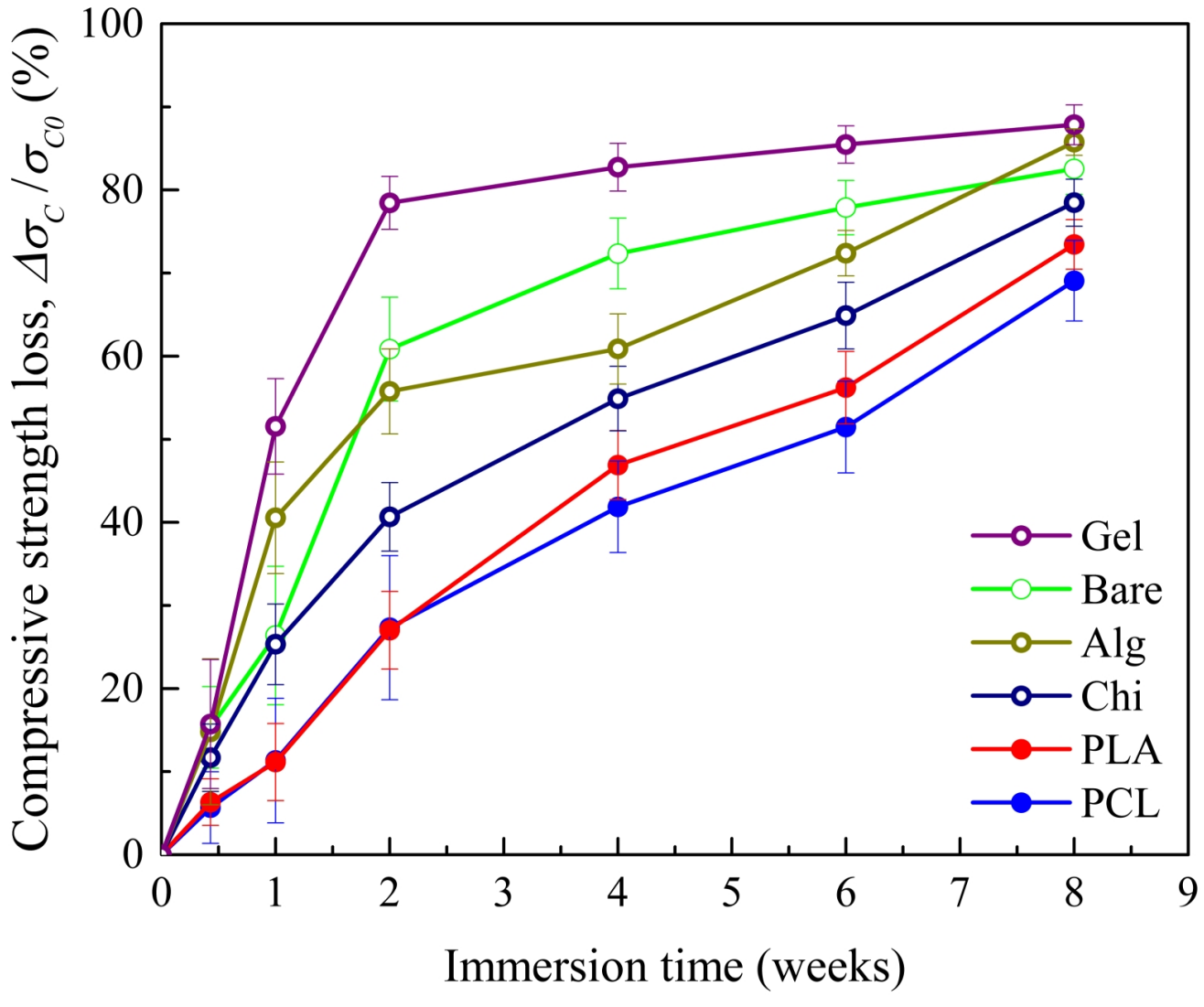
Compressive strength loss, $\Delta\sigma_C/\sigma_{C0}$ (%)
100
80
60
40
20
0
0
1
2
3
4
5
6
7
8
9
Immersion time (weeks)
Gel
Bare
Alg
Chi
PLA
PCL

a)

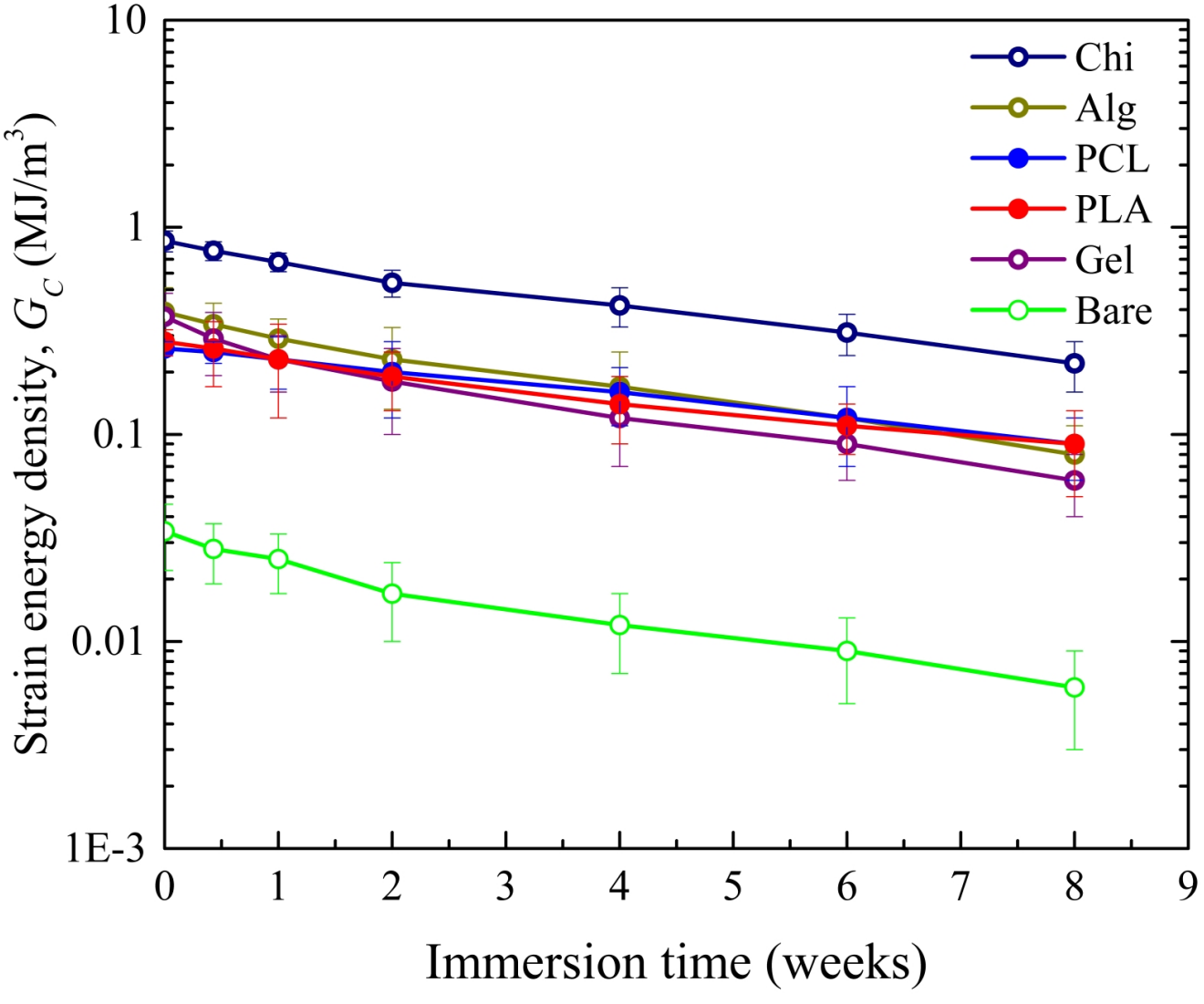
10
1
0.1
0.01
1E-3
0
1
2
3
4
5
6
7
8
9
Strain energy density, G_C (MJ/m^3)
Immersion time (weeks)
Chi
Alg
PCL
PLA
Gel
Bare

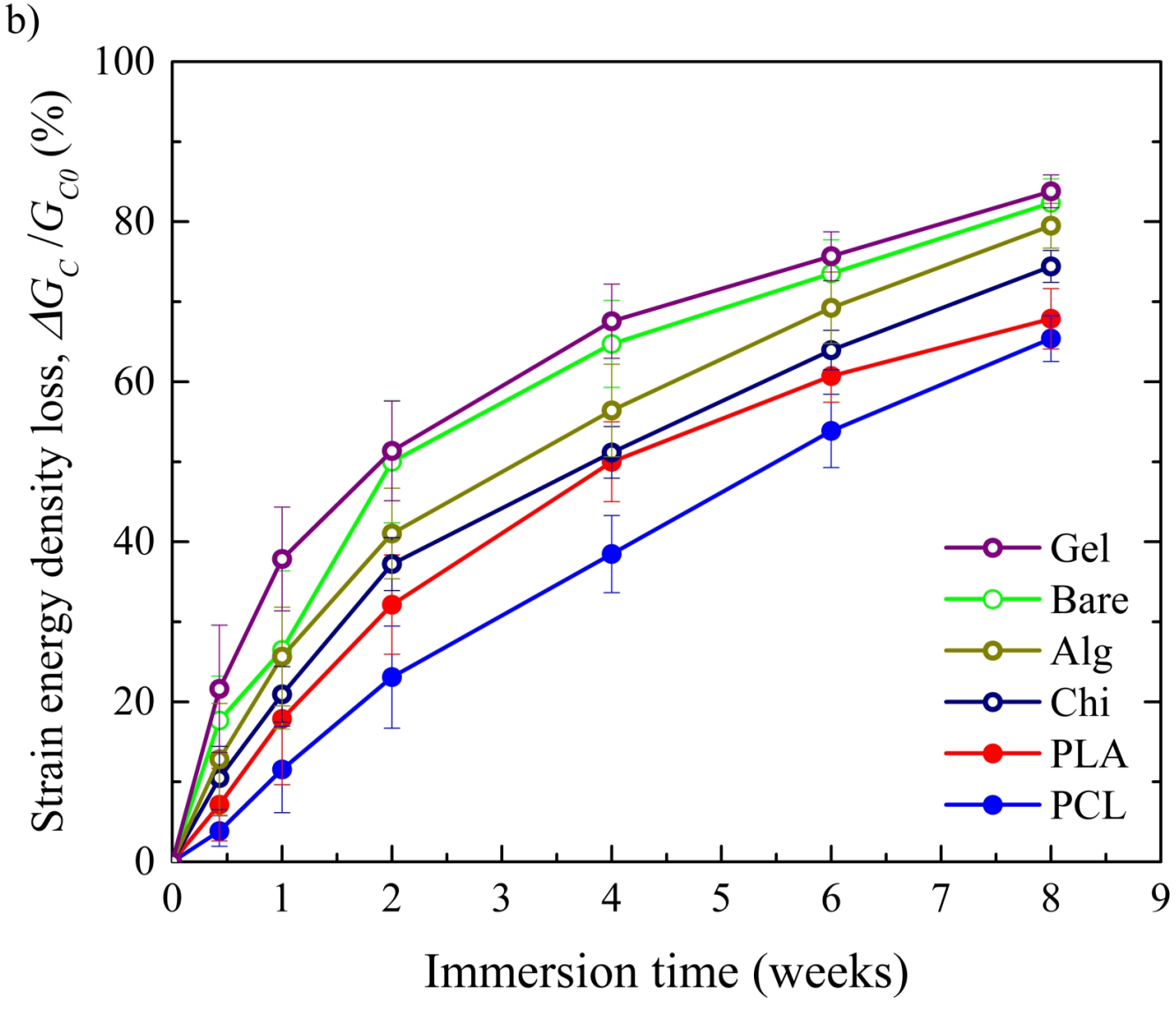
b)
Strain energy density loss, $\Delta G_C / G_{C0}$ (%)
100
80
60
40
20
0
0
1
2
3
4
5
6
7
8
9
Immersion time (weeks)
Gel
Bare
Alg
Chi
PLA
PCL

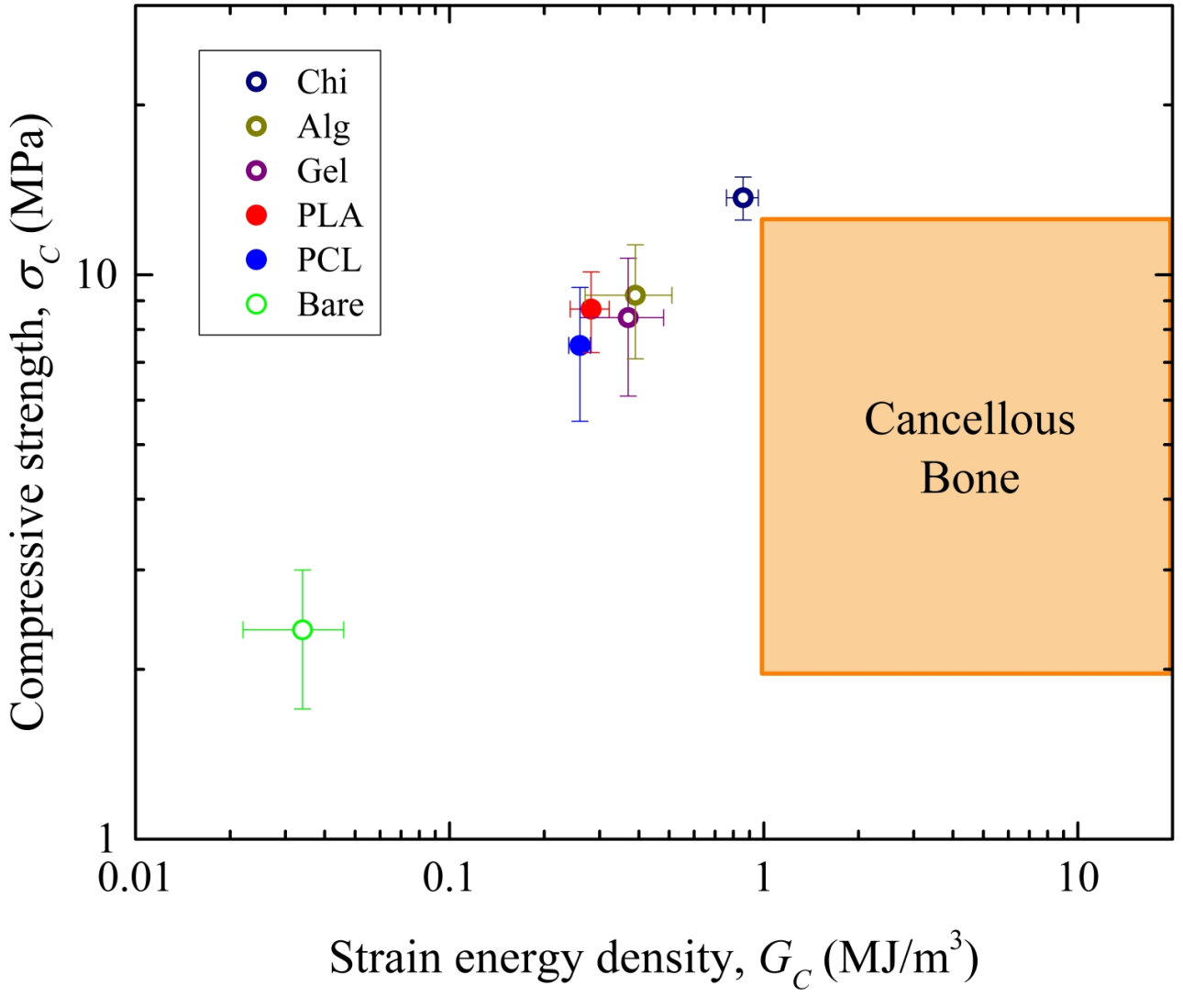
Chi
Alg
Gel
PLA
PCL
Bare
Cancellous
Bone
Compressive strength, σ_C (MPa)
10
1
0.01
0.1
1
10
Strain energy density, G_C (MJ/m^3)